

ABSTRACT

LOPEZ, VICTORIA MARIE. Commercial Food Waste Feedstock Characterization for Anaerobic Digestion. (Under the direction of Dr. Morton Barlaz.)

The solid waste management industry is actively pursuing options for landfill diversion. Large scale anaerobic digestion has increasingly become a viable option for organics diversion because biogas and digestate are valuable energy and nutrient byproducts from organics treatment in an anaerobic digester. Organics diversion has become predominant in many countries due to the energy potential and methane mitigation involved with food waste treatment by anaerobic digestion. Currently, there is little information on the characterization of commercial food waste sources or the effect of waste particle size on methane yield.

The objective of this research was to characterize four commercial food waste sources, (1) university dining hall pre and post-consumer waste, (2) waste resulting from prepared foods and leftover produce at a grocery store, (3) pre and post-consumer food waste from a hotel and convention center, and (4) food preparation waste from a restaurant. Each food waste sample was tested in triplicate lab-scale anaerobic digesters after shredding and after shredding and grinding to a fine particle size. Digesters were inoculated with well decomposed residential refuse to initiate methane generation. Wastes were characterized by measurement of substrate cellulose, hemicellulose, lignin, starch, protein, lipid and volatile solids content before and after anaerobic digestion.

On average, methane yields varied between about 340 and 500 ml CH₄/dry gm as reported in previous literature. It was determined that there is no significant effect of particle size on cumulative methane yield for any of the tested substrates. There was a significant

difference in lag time for both hotel waste and restaurant waste due to particle size, a trend not exhibited by the university and grocery wastes. In both feedstocks, pumpable waste resulted in a prolonged lag time. Also, there was a significant difference in methanation period for hotel waste tested. Specifically, pumpable hotel waste required a longer methanation time than the shredded hotel waste. Food waste with the highest lipid content was correlated with the lowest maximum methane production rates and the lowest lipid content food waste was correlated with the highest maximum methane production rates. Also, food waste with the lowest lipid content was correlated with the lowest lag time.

The waste characterization data obtained through this research will increase the predictability of biogas yields in digester facilities. Also, comparisons of methane yields with and without grinding will provide insight into the importance of this step in laboratory testing.

© Copyright 2015 Victoria Marie Lopez

All Rights Reserved

Commercial Food Waste Feedstock Characterization for Anaerobic Digestion

by
Victoria Marie Lopez

A thesis submitted to the Graduate Faculty of
North Carolina State University
in partial fulfillment of the
requirements for the degree of
Master of Science

Environmental Engineering

Raleigh, North Carolina

2015

APPROVED BY:

Dr. Morton Barlaz
Committee Chair

Dr. Francis de los Reyes

Dr. Joseph DeCarolis

BIOGRAPHY

Victoria Lopez began her engineering career at Florida State University while pursuing her undergraduate studies in Civil Engineering. Her passion for environmental engineering began during an undergraduate student exchange in Sweden where she compared the solid waste management practices of Sweden and the United States as a research topic. Directly after graduation, Victoria sought her Master of Science in Environmental Engineering at the NCSU Department of Civil, Construction, and Environmental Engineering. Victoria looks forward to practicing environmental process engineering as a professional engineer in order to optimize sustainable water, wastewater, and solid waste management practices.

ACKNOWLEDGMENTS

Special thanks to all advisers, fellow researchers, undergraduate research assistants, and food waste donors including, but not limited to: Dr. Morton Barlaz, Dr. Francis de los Reyes, Dr. Joseph DeCarolis, David Black, Dr. Lisa Castellano, Chris Westmoreland, Kris Malpico Blanco, Xiaoming Wang, Wenjie Sun, Johnsie Lang, Florentino de la Cruz, Joe Weaver, North Carolina State University Dining Services, The Sheraton Imperial Hotel & Convention Center, The Irregardless Café, and Weaver Street Market.

TABLE OF CONTENTS

LIST OF TABLES	v
LIST OF FIGURES	vi
INTRODUCTION	1
MATERIALS AND METHODS	10
Experimental Design	10
Feedstock Collection and Inoculum Preparation	11
Reactor Construction and Filling	12
Reactor Operation and Sampling	13
Analytical Methods	15
<i>Solids Analysis</i>	15
<i>Gas Analysis</i>	17
<i>Leachate Analysis</i>	18
<i>Data Analysis</i>	18
RESULTS AND DISCUSSION	21
Differentiation between Starch and Cellulose Measurement	21
Feedstock Chemical Characterization	24
Methane Production from Food Waste	27
Leachate Quality	37
Digested Solid Chemical Characterization	43
CONCLUSIONS	45
RECOMMENDATIONS	46
REFERENCES	47
APPENDICES	50
Appendix A Cumulative methane yield summary	51
Appendix B Leachate NH₃-N and PO₃ data for reactor batch 1	52
Appendix C Leachate NH₃-N and PO₃ data for reactor batch 2	53
Appendix D Lag time, methanation period, peak methane production rate, and lipid content in food waste reactors	54

LIST OF TABLES

Table 1 Summary of food waste methane yields reported in the literature	5
Table 2 Reactors used to determine the effect of commercial food waste type and particle size on methane production	11
Table 3 Summary of reactor contents.....	14
Table 4 Organic compound formulas and theoretical methane potential	19
Table 5 Cellulose and starch differentiation experiment plan	23
Table 6 Raw feedstock chemical characterization	26
Table 7 Average cumulative methane yield from the four food wastes tested.....	30
Table 8 Lab scale decay rate from the four food wastes tested	30
Table 9 Total reactor methane attributed to inoculum seed for the four food wastes tested...	36
Table 10 Reactor shutdown VFA concentrations	40
Table 11 Average digested solid chemical characterization for each triplicate reactor set.....	44

LIST OF FIGURES

Figure 1 Solids analysis process flow for raw food waste	15
Figure 2 Correlation between lipids and lag time, methanation time, and peak methane generation rate in food waste reactor studies	31
Figure 3 pH, methane production rate, cumulative methane yield, and COD plots for shredded and pumpable grocery store waste	32
Figure 4 pH, methane production rate, cumulative methane yield, and COD plots for shredded and pumpable university dining hall waste.....	33
Figure 5 pH, methane production rate, cumulative methane yield, and COD plots for shredded and pumpable hotel and convention center waste	34
Figure 6 pH, methane production rate, cumulative methane yield, and COD plots for shredded and pumpable restaurant waste	35
Figure 7 Leachate NH ₃ -N at reactor startup (first time point), peak methane generation (second time point), and reactor shutdown (third time point)	41
Figure 8 Leachate PO ₄ at reactor startup (first time point), peak methane generation (second time point), and reactor shutdown (third time point)	42

INTRODUCTION

The U.S. EPA estimates that 251 million tons of municipal solid waste (MSW) were generated in the U.S. in 2012 and that over 50% of this waste was disposed in landfills (EPA, 2012). As the quantity of materials recycled has increased, food waste has become the next logical waste component to target for diversion from landfills. Food waste is estimated to make up 14.5% of the MSW generated in the U.S. and it is both a rapidly degradable and high methane yield substrate. These characteristics make it a particularly appealing target for diversion since significant methane is produced prior to installation of a gas collection system. For example, using a decay rate of 0.14 yr^{-1} , as suggested by de la Cruz and Barlaz (2010), 24.6 % of the methane potential of food waste would be produced in the first two years when a gas collection system is least likely to be in place.

One alternative for food waste diversion is anaerobic digestion (AD). Currently, large scale anaerobic digestion (AD) is a viable option for organics diversion because biogas, a valuable energy source, is produced and the digestate can be used as a soil amendment which offsets the addition of mineral fertilizers. AD of food waste has the potential to offset grid energy as well as reduce the quantity of methane released to the atmosphere as capture efficiencies in AD systems are considerably higher than in landfills. AD has become a common practice in Europe due to waste directives requiring European Union Member States to reduce the quantity of municipal organic waste disposed in landfills (EEA, 2009). It is known that large-scale AD of organics is feasible, however the implementation of AD as compared to landfills is not cost competitive in the U.S. (Yazdani et al., 2012). With the exception of a few cities, AD implementation within the U.S. has been limited.

Recently, there have been several efforts to promote organics diversion from landfills in the U.S. For example, in 2014, Massachusetts established the most ambitious commercial food waste disposal ban in the U.S (DEP, 2014). This ban requires businesses and institutions that dispose of at least one ton of food per week to treat their waste through composting or anaerobic digestion, or to donate the unused food to charity or to farms for animal feed. In California, the Greenhouse Gas Reduction Fund has allocated \$19.5 million in grants to promote an increase in recycling and diversion of organics from landfills (<http://www.calrecycle.ca.gov/NewsRoom/2014/11Nov/27.htm>, April 2015). This program has awarded five grants to composting and AD facilities to support expansion or startup of food waste treatment in the state. In March 2014, the White House announced the *Climate Change Action Plan-Strategy to Reduce Methane Emissions*. In this plan, the U.S. Department of Agriculture (USDA), the U.S. Environmental Protection Agency (EPA) and the U.S. Department of Energy (DOE) agreed to collaborate with industry leaders to outline a biogas roadmap (U.S. Department of Agriculture, 2014). Recently, the U.S. EPA classified biogas produced from food waste as cellulosic biofuel under the Renewable Fuel Standard (RFS) (U.S. Department of Agriculture, 2014). The RFS increase the economic feasibility of food waste AD because biogas producers are able to generate Renewable Identification Numbers (RINs) which may in turn be sold to fuel refiners, blenders, and importers to show that they have sold renewable fuels to meet renewable fuel volume obligations.

There have been numerous studies to measure the methane potential of food waste and measured methane yields range from 130 to 630 m³/Mg volatile solids (VS) (Table 1). This range could be due to a variety of factors including the chemical composition of the

food waste feedstock, feedstock particle size, reactor configuration during testing, or the adequacy of the digestion period to reach complete methane potential. In some of the studies listed in Table 1, for example, Qiao et al. (2011) and Browne and Murphy (2013), it is not clear whether the test duration was sufficient to measure the maximum methane potential of the waste. Continuous reactor systems, as opposed to batch systems, make it difficult to determine whether food waste substrates have reached their maximum methane potential due to continuous reactor feeding. A study by Agyeman and Tao (2014) showed that in the case of hotel restaurant substrate, the methane yield increased with a decrease in particle size over a 178 day monitoring period in a stirred reactor system.

Commercial food waste represents the most likely feedstock for AD facilities because it is generated in large quantities at a few locations as opposed to residential food waste which is generated in smaller quantities at a large number of locations. In addition, it may be easier to reduce the presence of contaminants in commercial food waste due to the smaller number of waste generators. Feedstock purity is important if the digestate is to be used for land application after digestion.

Currently, there is little information on the methane potential of specific commercial food waste sources determined by lab-scale reactor experiments. As shown in Table 1, there is ample research indicating the methane potential of specific food types or mixtures of commercial food waste collected on a pickup route. However, only one study by Qiao et al. (2011) presented data comparing the methane potential of different commercial food waste feedstocks. In general, methane potential measurements have been performed in relatively small systems. Food waste methane yield studies performed with a larger reactor size and a

high solid to liquid ratio, as opposed to biochemical methane potential (BMP) tests, more closely simulate commercial digester conditions.

The objective of this research was to characterize the methane yield and chemical composition of commercial food waste from four sources including grocery, restaurant, hotel, and dining hall waste. The decomposition of food waste under anaerobic conditions was characterized by measurement of the methane yield and chemical composition of each waste (starch, cellulose, hemicellulose, lignin, protein, and lipid) prior to and after decomposition. In addition, each waste was tested after shredding and after processing through a 0.5 cm diameter aperture food grinder to evaluate the effect of particle size on decomposition. The data generated in this study will provide useful information on the characteristics of individual commercial wastes that may be processed by AD.

Table 1 Summary of food waste methane yields reported in the literature

Food Type	Particle Size	Inocula	Reactor Type	Temp.	Digestion Period (d)	Complete degradation? ^a	Methane Yield (m ³ /Mg VS)	MC % ^d	VS %DryW	Reference
Cooked meat	Ground size NR	Digester sludge from sanitary treatment plant	125 mL BMP	Mesophilic	30	Y	482	47	97	(Cho et al., 1995)
Boiled rice	Ground size NR	Digester sludge from sanitary treatment plant	125 mL BMP	Mesophilic	31	Y	294	65	99	(Cho et al., 1995)
Fresh cabbage	Ground size NR	Digester sludge from sanitary treatment plant	125 mL BMP	Mesophilic	32	Y	277	95	84	(Cho et al., 1995)
Korean	Ground size NR	Digester sludge from sanitary treatment plant	125 mL BMP	Mesophilic	33	Y	472	74	95	(Cho et al., 1995)
Korean	2-4 mm	Lab scale co-digestion seed	500 mL BMP	Mesophilic	40	Y	489	85	88	(Heo et al., 2004)
Residential	<5 cm	Well decomposed refuse	2 L Batch	Mesophilic	~188	Y	320	NR	93.8	(Eleazer et al., 1997)
Mixed commercial	NR	Digester sludge from a municipal wastewater plant	500 mL Batch	Thermophilic	28	Y	445	70	83	(Zhang et al., 2007)

Table 1 Continued

Food Type	Particle Size	Inocula	Reactor Type	Temp.	Digestion Period (d)	Complete degradation? ^a	Methane Yield (m ³ /Mg VS)	MC % ^d	VS %DryW	Reference
University canteen	Crushed size NR	Lab scale co-digestion seed	250 mL BMP	Mesophilic	14	NR	531	80.2 ₉	86	(Qiao et al., 2011)
Farmers market fruit & vegetables	Crushed size NR	Lab scale co-digestion seed	250 mL BMP	Mesophilic	14	NR	281	90.8 ₅	84	(Qiao et al., 2011)
University canteen	Minced size NR	Farm digester sludge (80% cattle slurry and 20% grease trap waste)	0.5 L BMP	Mesophilic	30	NR	415	70.6	95.3	(Browne and Murphy, 2013)
University canteen	Minced size NR	Farm digester sludge (80% cattle slurry and 20% grease trap waste)	5 L BMP	Mesophilic	30	NR	357	70.6	95.3	(Browne and Murphy, 2013)
Hotel restaurant	<2.5 mm	Digester sludge from a wastewater plant (50%) and dairy manure (50%)	2 L Complete mix continuous	Mesophilic	178	NR	630	NR	29.3 ^c	(Agyeman and Tao, 2014)

Table 1 Continued

Food Type	Particle Size	Inocula	Reactor Type	Temp.	Digestion Period (d)	Complete degradation? ^a	Methane Yield (m ³ /Mg VS)	MC % ^d	VS %DryW	Reference
Hotel restaurant	<4 mm	Digester sludge from a wastewater plant (50%) and dairy manure (50%)	2 L Complete mix continuous	Mesophilic	178	NR	560	NR	29.3 ^c	(Agyeman and Tao, 2014)
Hotel restaurant	<8 mm	Digester sludge from a wastewater plant (50%) and dairy manure (50%)	2-L Complete mix continuous	Mesophilic	178	NR	470	NR	29.3 ^c	(Agyeman and Tao, 2014)
Research institution	Macerated size NR	Digester sludge from an upflow anaerobic sludge blanket reactor	2-L Complete Mix Batch Reactor	Undefined	60	NR	338	75	93	(Mohan and Bindhu, 2008)
Research institution	Macerated size NR	Digester sludge from an upflow anaerobic sludge blanket reactor	7 L Single stage continuous	Undefined	15	NR	288	75	93	(Mohan and Bindhu, 2008)

Table 1 Continued

Food Type	Particle Size	Inocula	Reactor Type	Temp.	Digestion Period (d)	Complete degradation? ^a	Methane Yield (m ³ /Mg VS)	MC % ^d	VS %DryW	Reference
Research institution	Macerated size NR	Digester sludge from an upflow anaerobic sludge blanket reactor	2-L Two stage complete mix continuous	Undefined	10	NR	219	75	93	(Mohan and Bindhu, 2008)
Single family house in paper bag	Disc screen size NR	Digester sludge from Swedish biogas plants	35-L Complete mix semi-continuous pilot	Thermophilic	15	NR	344	71.5	89	(Davidsson et al., 2007)
Apartment block in paper bag	Disc screen size NR	Digester sludge from Swedish biogas plants	35-L Complete mix semi-continuous pilot	Thermophilic	15	NR	349	72	87	(Davidsson et al., 2007)
Single family house in paper bag	Screw press size NR	Digester sludge from Swedish biogas plants	35-L Complete mix semi-continuous pilot	Thermophilic	15	NR	275	71	92	(Davidsson et al., 2007)
Single family house in paper bag	Shredder & magnet size NR	Digester sludge from Swedish biogas plants	35-L Complete mix semi-continuous pilot	Thermophilic	15	NR	289	72	92	(Davidsson et al., 2007)

Table 1 Continued

Food Type	Particle Size	Inocula	Reactor Type	Temp.	Digestion Period (d)	Complete degradation? ^a	Methane Yield (m ³ /Mg VS)	MC % ^d	VS %DryW	Reference
Apartment block in paper bag	Piston press size NR	Digester sludge from Swedish biogas plants	35-L Complete mix semi-continuous pilot	Thermophilic	15	NR	284	68	87	(Davidsson et al., 2007)
Restaurant, grocery, produce market	Slurry, passed through a 0.065 in aperture	Full scale digester sludge	30-L Complete mix semi-continuous	Mesophilic	10	NR	334	67	89.9	(Gray et al., 2008)
Residential	NR	Well decomposed refuse leachate	8-L Batch	Mesophilic	~ 320	Y	225	NR ^b	NR	(Staley et al., 2006)
Synthetic OFMSW	1 mm	Digester sludge from a wastewater plant	5-L Semi-continuous	Thermophilic	15	NR	130	72.5	71	(Fdez-Güelfo et al., 2011)

a. Complete degradation is indicated by minimal or non-measurable methane generation at the end of reactor operation

b. VS was not reported so an average VS content of 92% was used to calculate methane production per gram of VS

c. Reported on wet weight basis

d. MC is defined as moisture content

NR indicates data not reported

MATERIALS AND METHODS

Experimental Design

The objective of this research was to characterize the methane yield and chemical composition of individual commercial food wastes. Four commercial food wastes were tested including waste generated at a restaurant, grocery store, hotel, and a university dining hall. These wastes include both pre and post-consumer food waste. Each feedstock was characterized and digested in triplicate 8-L batch reactors after either shredding or shredding and then grinding to a slurry that could be moved by pumping (Table 2). Each reactor was filled with a 7:3 volumetric mixture of well degraded MSW inoculum and food waste to insure the stable onset of biodegradation. Reactors were incubated at 37 °C to enhance the rate of microbial biodegradation. Blank reactors with MSW inoculum only were operated to measure background methane production from the MSW seed. Each reactor was operated until methane production was either no longer measurable or the methane yield had changed by less than 1% over the previous 3 weeks.

The experiment was designed to simulate anaerobic digester conditions to determine the ultimate methane yield of each commercial feedstock at two different particle sizes. Additionally, the chemical composition (starch, cellulose, hemicellulose, lignin, protein, and lipid) of each feedstock was determined before and after digestion to estimate the volume of methane attributable to each compound.

Table 2 Reactors used to determine the effect of commercial food waste type and particle size on methane production

Reactor	Description
B1,B2,B3,B4,B5,B6	MSW Inoculum Seed Control Blanks
GS1,GS3 ^a	Grocery Store Shredded
GP1,GP2,GP3	Grocery Store Pumpable
US1,US2,US3	University Dining Hall Shredded
UP1,UP2,UP3	University Dining Hall Pumpable
HS1,HS2,HS3	Hotel and Conference Center Shredded
HP1,HP2,HP3	Hotel and Conference Center Pumpable
RS1,RS2,RS3	Restaurant Shredded
RP1,RP2,RP3	Restaurant Pumpable

^a. Reactor GS2 was removed from the data set due to a gas leak early in reactor operation.

Feedstock Collection and Inoculum Preparation

Food waste was collected from businesses and institutions that separate organics as part of their daily kitchen procedures. University dining hall food waste was collected from North Carolina State University’s largest campus dining hall. Approximately 30-L of post-consumer dining hall waste was collected on four consecutive weekdays. By visual inspection, the university waste mostly consisted of bread, meat, cheese, and fruit and vegetable waste. 40-L of grocery store waste was sampled from Weaver Street Market in Carrboro, North Carolina. This waste was obtained during one sampling weekday and was sourced from hot bar buffet food remains and discarded produce. This grocery waste mostly consisted of discarded vegetables from the produce aisle and a mass of grits with French toast from the hot bar. Thirty L of hotel food waste was sampled from the Sheraton Imperial

Hotel and Convention Center in Durham, North Carolina. This sample was obtained on one weekday and consisted of pre- and post-consumer food from the kitchen. The majority of the waste consisted of large beef tenderloins, cheese, sour cream, and potato peels. The restaurant waste sample was collected from The Irregardless Café in Raleigh, North Carolina. Approximately 30-L of food preparation waste was collected on three separate weekdays. The food preparation waste consisted mostly of discarded raw vegetables and raw meat with bone scraps. All collections occurred on weekdays and non-holidays.

Collected food waste samples were frozen immediately upon arrival in the lab until further preprocessing. Each frozen feedstock was shredded with a slow-speed, high-torque shredder (Shredpax AZ-7H). To achieve a slurry or pumpable material, part of the shredded feedstock was further ground through a 0.5 cm diameter aperture meat grinder (Northern Industrial, Burnsville, MN). Once shredded or ground, food waste samples were pre-weighed, stored in Ziploc bags, and frozen until preparation for reactor loading. Samples were thawed in a refrigerator for 2 days prior to reactor loading.

Well degraded anaerobic MSW was used as a seed to initiate decomposition. This MSW was obtained from a ~300-L reactor maintained in the Environmental Engineering Lab at North Carolina State University.

Reactor Construction and Filling

The reactors consisted of an 8-L polypropylene jar with an airtight screw cap (U.S. Plastics Corp., Lima, OH), a 2-L intravenous bag (Baxter Healthcare, Deerfield, IL) for

leachate collection and recirculation, and two 25-L flexfoil gas collection bags (SKC Corp., Houston, TX).

At reactor startup, the well degraded MSW inoculum and the thawed food waste samples were mixed in a bin to reach a 7:3 volumetric mixture of well degraded MSW to food waste. The 8-L reactors were filled with this mixture and sealed. Once sealed, the headspace was sparged with N₂ gas to remove any residual O₂. After the food waste moisture drained into the recirculation bags, sufficient deionized water was added to obtain approximately 500 mL of leachate. A summary of the contents of each reactor is presented in Table 3.

Reactor Operation and Sampling

Reactors were operated to maximize the extent of decomposition. This included the inoculum described above, incubation in a room at 37°C and leachate neutralization. Collected leachate was neutralized with 2 N NaOH every other day until a neutral pH (6.8-7.8) was reached. Once the pH was neutral and methane production was initiated, leachate recirculation was reduced to weekly and neutralization was not necessary. Leachate samples were collected for chemical oxygen demand (COD) analysis weekly to biweekly. Soluble NH₃-N and PO₄-P concentrations were measured during the reactor startup phase, peak methane generation phase, and reactor shutdown phase to ensure that nutrient levels of at least 5 mg of P/L and 100 mg of N/L were maintained for proper microorganism growth (Eleazer et al., 1997). Flex-foil gas collection bags were analyzed for biogas composition and volume weekly to biweekly based on gas production rates.

Table 3 Summary of reactor contents

Reactor	Mass Food Waste (dry g)	Mass Inoculum (dry g)	Liquid Added (mL)
B1	0.0	814.0	0
B2	0.0	801.4	0
B3	0.0	817.7	0
GS1 ^b	98.9	492.8	60
GS3	103.7	488.8	60
GP1	123.9	511.0	120
GP2	129.2	502.3	140
GP3	125.0	488.1	120
US1	389.4	471.3	60
US2	372.5	479.8	60
US3	378.9	476.7	60
UP1	390.1	482.4	200
UP2	400.6	475.8	120
UP3	392.8	492.2	100
B4	0.0	472.2	0
B5	0.0	519.3	120
B6	0.0	485.8	0
HS1	260.9	400.3	0
HS2	230.5	359.0	0
HS3	273.2	339.0	420
HP1	364.7	349.0	0
HP2	436.7	407.2	240
HP3	445.6	419.5	0
RS1	124.8	393.6	360
RS2	128.2	387.6	540
RS3	127.4	393.1	420
RP1	211.8	402.8	0
RP2	203.3	380.3	540
RP3	211.1	426.8	0

Analytical Methods

Solids Analysis

Solids analyses (lipids or lipophilic extractives, starch, cellulose, hemicellulose, lignin, volatile solids, total carbon, and total nitrogen) were performed on all initial feedstocks and inoculum as well as digested solid residuals. An overview of the solids analysis procedure for the fresh food waste is presented in Figure 1,

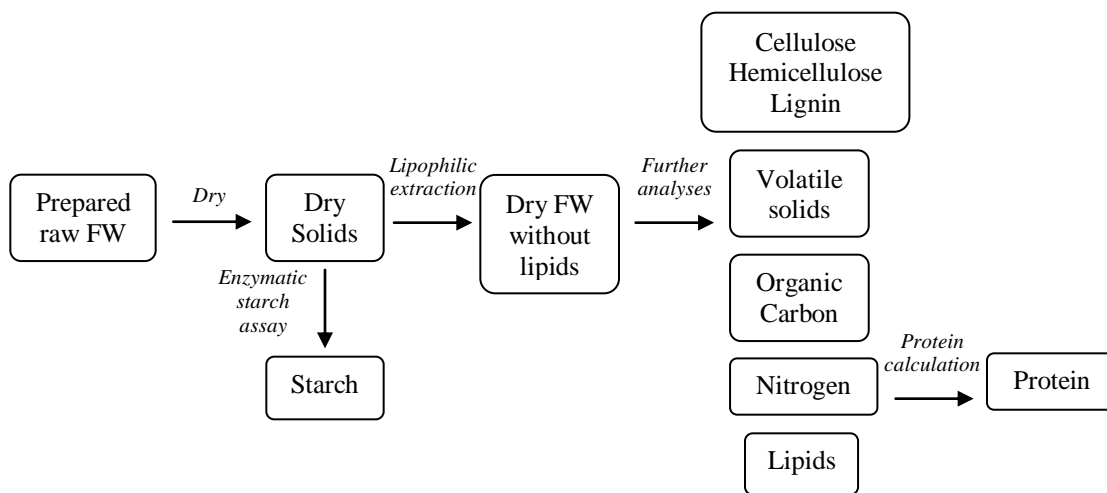


Figure 1 Solids analysis process flow for raw food waste

Prior to analysis for volatile solids, cellulose, hemicellulose, lignin, organic C and N, it was necessary to grind the dry solids in a wiley mill to pass a 1 mm screen. However, the high fat content of the solids clogged the wiley mill. As such, it was necessary to extract the food waste prior to solids analysis. This partial lipid extraction was accomplished by washing the dry food waste with a 2:1 ratio of toluene to ethanol. All solids data obtained post-lipophilic extraction was corrected for the loss of lipids in the dry food waste solids. Because the extraction removed lipophilic material that contained organic C, it was necessary to

calculate the organic C of the initial substrate based on the measured organic C plus the organic C in the extracted material. The organic C in the extracted material was calculated by assuming the C content of fats as given in the results.

Digested solids were directly dried, ground in a wiley mill to pass a 1 mm screen, and then analyzed for starch, volatile solids, total carbon, total nitrogen, lipids, cellulose, hemicellulose, and lignin without extracting the lipids first because this step was not necessary. Again, all results are presented as a percentage of the initial dry weight of the sample prior to lipid extraction.

Cellulose, hemicellulose, and lignin (CHL) analyses began with a Soxhlet extraction of ~1g of dry sample with a 2:1 volumetric ratio of toluene/ethanol in a ST 255 Soxtec Semi-automated solvent extraction unit (Foss, MN). A two-stage acid hydrolysis was performed on a known quantity of this sample. Arabinose, galactose, glucose, mannose, and xylose sugars were released by the acid digestion and analyzed by HPLC using an ICS 2500 electrochemical detector (Dionex, Sunnyvale, CA). Glucose was converted to cellulose and other sugars to hemicelluloses by anhydro correction. Klason lignin was determined by ignition of the remaining solids after acid hydrolysis at 550°C for 2 h (De la Cruz et al., 2014).

The lipid content was reported by direct determination of the lipid weight extracted from the sample during Soxhlet extraction using a 2:1 ratio of toluene to ethanol and a process of boiling (20 min), rinsing (90 min), recovering (5 min) and drying (3 min) the sample. Starch analyses were performed by Cumberland Valley Analytical Services in Hagerstown, MD. The starch assay included a 2-stage, heat-stable, α -amylase and

amyloglucosidase hydrolysis using an acetate buffer in the gelatinization solution (Hall, 2008). Total carbon and total nitrogen were analyzed with a CHN analyzer (Perkin-Elmer PE 2400 Elemental Analyzer). This total carbon value represents total organic carbon, as samples were washed with 1 N HCl to remove inorganic carbon prior to analysis (Ryba and Burgess, 2002). The carbon content was also corrected for the loss of carbon due to lipid extraction of the raw food waste feedstocks as described above. Protein content was calculated by multiplying the organic nitrogen by a factor of 6.25, where organic nitrogen was assumed to be the difference between total nitrogen and soluble ammonia nitrogen (Hansen et al., 1998). There is uncertainty in this protein estimate as the total nitrogen value contains non-protein nitrogen attributed to lignin. Volatile solid content was determined by weight loss during ignition at 550 °C for 2 hours (Wang et al., 2013).

Gas Analysis

Approximately 10 mL of gas were used to analyze for CH₄, CO₂, N₂, and O₂ using an SRI gas chromatograph equipped with a thermal conductivity detector (TCD) and a CTR-1 column (Alltech Co., Deerfield IL). The carrier gas was 88 mL He/min at an oven temperature of 75°C. Gas volume was measured by evacuating the gas into a cylinder of a known volume and monitoring the pressure difference (Staley et al., 2006). Measured gas volumes were corrected to standard temperature and pressure. Food waste methane production rates and yields were corrected for the background methane produced from inoculum. These methane production rates represent the quantity of methane attributable to

food waste on the assumption that methane produced from the inoculum in the inoculum only reactors was the same in reactors that contained a mixture of food waste and inoculum.

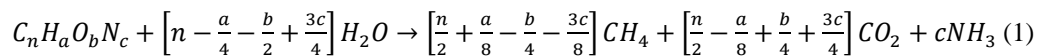
Leachate Analysis

Soluble COD, NH₃-N and PO₄-P concentrations were determined using Hach Kits (Hach Co., Loveland, CO).

Selected volatile fatty acid (VFA) analyses were performed on leachate from grocery and hotel waste reactors. This assay was used to determine individual concentrations of acetic, propionic, n-butyric, isobutyric, valeric, and isovaleric, i-caproic, and hexanoic acids. Before analysis, samples were centrifuged, filtered, and acidified. Each acid was converted to a volatile form prior to injection into the gas chromatograph which was equipped with a flame ionization detector.

Data Analysis

The theoretical quantity of methane (Table 4) that can be produced from cellulose and starch, hemicellulose, protein, and lipids in the system was calculated using the Buswell Equation (Parkin and Owen, 1986) as shown in equation 1:



The chemical formulae for each compound measured (cellulose and starch, hemicellulose, protein, and lipids) and input into the Buswell Equation are shown in Table 4.

Table 4 Organic compound formulas and theoretical methane potential

Organic Compound	Chemical Composition Formula	Theoretical CH ₄ Yield (L CH ₄ /g)
Cellulose, Starch ^a	C ₆ H ₁₀ O ₅	0.4148
Hemicellulose ^b	C ₅ H ₈ O ₄	0.4242
Protein ^a	C ₅ H ₇ NO ₂	0.4955
Lipid ^a	C ₅₇ H ₁₀₄ O ₆	1.0135

a. Composition formula was obtained from Christensen (2011)

b. Composition formula was obtained from Yazdani (2010)

A methane potential mass balance will be performed using equation 2 for each reactor. The methane potential of raw solids and digested solids will be determined using carbohydrate, protein, and lipid data presented with the results and applying these quantities to methane potentials obtained from equation 1 as given in Table 4.

The methane potential mass balance is shown in equation 2:

$$(CH_4 \text{ potential}_{raw \text{ solid}}) = (CH_4 \text{ potential}_{digested \text{ solid}}) + (CH_4 \text{ generated}) \quad (2)$$

where the methane potential of the solids is the sum of the methane potential of each measured compound.

Lab-scale decay rates (k_{lab}) determined for the food wastes tested in this study (Table 8) were determined by a method previously used to determine the lab-scale decay rate of food waste (de la Cruz and Barlaz, 2010). The lab scale decay rates were determined by inserting methane production data from food wastes into equation 3, a linear form of the first order decay equation (de la Cruz and Barlaz, 2010). Methane production data from the

reactor studies were fit to equation 3 to estimate k_{lab} by linear regression. All k_{lab} values were derived from the linear part of the plotted curve.

$$\ln(m_o - (m_{CH_4} + m_{CO_2})) = -kt + \ln(m_o) \quad (3)$$

RESULTS AND DISCUSSION

This section begins with a presentation of the plan to differentiate between starch and cellulose. As discussed in the introduction, this is important given the availability of renewable fuel credits for cellulosic methane that are not applied to methane generated from starch. This is followed by a chemical characterization of the food wastes tested, the methane production characteristics of each waste, and then leachate quality (COD, pH, NH₃-N, and PO₄).

At the time of this thesis submission, solids analyses were incomplete. As such, there are gaps in the data and text that will be updated as soon as results are available and reported in a journal.

Differentiation between Starch and Cellulose Measurement

Both cellulose and starch are composed of the glucose polymer; however the units are linked differently (Madigan et al., 2008). Cellulose is structured with β -1, 4 linkages whereas starch contains α -1, 4 linkages. The quantification of starch and cellulose was of concern for this research because the current cellulose and hemicellulose assay determines cellulose content by anhydrous correction of glucose released by acid hydrolysis. This acid hydrolysis is expected to release starch, also as glucose, and this glucose would be measured as cellulose which would result in the measured cellulose actually representing the sum of cellulose plus starch.

To evaluate the extent to which starch is being measured as cellulose in our cellulose assay, a corn starch standard will be tested for both cellulose (by acid hydrolysis and HPLC)

and starch (enzymatic hydrolysis). A series of tests will be conducted as described in Table 5.

Preliminary results, as shown in Table 5, indicate that analytical grade corn starch consists of 91.8% dry weight starch and 90.0% dry weight cellulose. This indicates that the cellulose analysis is capturing starch as cellulose, thus over quantifying the cellulosic content of food waste. Based on these results, the reported cellulose content in this manuscript is the measured cellulose content minus the independently measured starch content.

Table 5 Cellulose and starch differentiation experiment plan

Test	Description	C(ac) ^a or S(en) ^b Assay	Soxhlet Extraction	Objective	Cellulose (%)	Starch (%)	Cellulose Reported (%) ^c
1	Corn starch standard (analytical grade)	C(ac) & S(en)	None	Indicates what percent of starch measured as cellulose	90.0	91.8	<0
2	Corn starch standard	C(ac)	Yes	Evaluate effect of Soxhlet extraction on behavior of starch in starch and cellulose analyses	ND	-	ND
3	Grocery shredded food waste	C(ac)	Yes	Indicates whether or not CHL values match previously run carbohydrate values	ND	-	ND
4	Grocery shredded food waste with a known cellulose content and corn starch standard to reach 50% cellulose total	C(ac)	Yes	Indicates if glucose coming from starch is measure in CHL analysis in a medium similar to food waste substrate	ND	-	ND

a. C(ac) represents cellulose measurement by acid hydrolysis

b. S(en) represents starch measurement by enzymatic hydrolysis

c. Reported cellulose content in this manuscript represents the measured cellulose content minus the independently measured starch content

ND indicates data not yet determined

Feedstock Chemical Characterization

The chemical characterization of each feedstock is shown in Table 6. All tested food waste contained a high moisture and volatile solids content as expected from the literature. An organic component balance was calculated by adding the sum of lipids, cellulose, hemicellulose, starch, lignin, and protein and dividing by the volatile solids content. If each material was perfectly characterized, this ratio would be equal to 1.0. As shown in Table 6, the organic component balance ranged from 0.82 to 0.96 which indicated that feedstock characterization was fairly effective at determining solids chemical composition.

It is evident that each waste varied in lipid, starch, cellulose, hemicellulose, lignin, and protein content. The lipid content is relatively high which is expected of food waste. While data on the extractive content of MSW samples has typically not been reported, anecdotally, values above 3% were rare. It should be noted however, that most of the experience with MSW analysis has been on decomposed as opposed to fresh samples where lipid consumption would have occurred.

The presence of lipids contributes to the methane potential of refuse, given their methane potential of 1,014 mL CH₄/g VS (Christensen, 2011). However, potential inhibitory affects due to high lipid loading make lipids a key factor of food waste feedstock quality. Previously, lipids have been reported to exhibit toxicity in 100 mL batch experiments with several lipid loading dilutions (Lou et al., 2012). In the Lou et al. (2012) study, a lag in methane production and an increased methanation time were attributed to lipid toxicity. Lipid inhibition was most noticeable for less diluted feedstock experiments. Despite the initial lag phase of lipid rich reactors, the substrate degraded effectively (Lou et al., 2012). This study

suggests that lipids should be the food waste chemical component of concern when designing for digester efficiency which aligns with the conclusions of a study by Neves et al. (2008).

The hotel food waste contained the highest protein and lipid content and the extent to which this affected methane production was evaluated with the methane production data. Visually, the hotel food waste was observed to have the highest concentrations of both meat and dairy products relative to the grocery, restaurant and university wastes. This is consistent with the elevated protein and lipid contents.

Table 6 Raw feedstock chemical characterization ^a

Substrate ^b	MC%	VS%	Lipid%	Starch%	Cellulose%	Hemicellulose%	Lignin%	Protein %	Org.C% ^c	N%	Organic Component Balance ^d
B	81.4	45.3	5.5	0.6	4.5	1.6	21.7	7.6	23.6	1.2	-
GS	87.1	94.2	27.0	16.4	10.6	3.5	3.5	18.6	48.2	3.0	0.85
GP	86.9	94.0	32.8	13.8	8.1	3.1	3.5	19.0	48.2	3.0	0.86
US	71.1	94.3	41.7	20.4	3.7	2.4	3.1	13.9	50.5	2.2	0.90
UP	71.9	94.3	39.5	17.0	6.9 ^e	2.5 ^e	3.1	15.7	50.5	2.5	0.90
B	86.2	29.6	4.1	0.3	ND	ND	ND	4.7	17.8	0.8	-
HS	72.7	96.1	44.2	13.3	3.0 ^e	1.6 ^e	0.0	26.5	56.2	4.2	0.92
HP	73.2	96.1	47.2	13.3	4.1 ^e	1.8 ^e	0.0	25.6	56.8	4.1	0.96
RS	84.5	90.9	38.3	2.7	8.0 ^e	4.1 ^e	0.1	22.3	50.1	3.6	0.83
RP	85.3	92.2	40.5	1.6	8.1 ^e	4.3 ^e	0.1	21.4	50.9	3.4	0.82

- a. Results are reported as a % of dry weight with the exception of moisture content (MC); ND indicates that data has not yet been determined
- b. B is MSW Inoculum Seed Control Blanks, GS is Grocery Store Shredded, GP is Grocery Store Pumpable, US is University Dining Hall Shredded, UP is University Dining Hall Pumpable, HS is Hotel and Conference Center Shredded, HP is Hotel and Conference Center Pumpable, RS is Restaurant Shredded, and RP is Restaurant Pumpable food waste reactors
- c. Because the extraction removed lipophilic material that contained organic C, it was necessary to calculate the organic C of the initial substrate based on the measured organic C plus the organic C in the extracted material. The organic C in the extracted material was calculated by assuming a C content of 77.4% of lipids by weight as given in Table 4.
- d. The organic component balance was calculated by adding the sum of lipids, cellulose, hemicellulose, starch, lignin, and protein and dividing by the volatile solids content.
- e. Data reported is preliminary. Further cellulose and hemicellulose data will be reported in the future.

Methane Production from Food Waste

The methane production characteristics of each substrate are presented in this section. Methane production rates and cumulative yields are illustrated in Figure 3 to Figure 6. In all cases, the methane production rates exhibited an increase followed by an asymptotic decrease. Peak methane generation rates ranged from 5 to 15 mL CH₄/day-dry g in the hotel, restaurant and university wastes but were as high as 30 mL CH₄/day-dry g in the grocery store waste.

Another characteristic of the rate curves is the lag time prior to methane production initiation. For this discussion, the lag time was defined as the time until the methane production rate was greater than or equal to 2.64 mL CH₄/g-d. This value corresponds to the time at which the methane generation rate began to exhibit a steep increase. The methanation period was defined as the amount of time in between the lag and a methane generation rate less than or equal to 1 mL CH₄/g-d on the decreasing side of the methane production rate curve. Using these definitions, measurement frequency reduces the precision of the reported lag and methanation times because gas measurements were typically weekly. Thus, there is an error of up to 6 days in the lag and methanation times.

T-tests ($p > 0.05$) confirm that there was a significant difference in lag time for both hotel waste and restaurant waste due to particle size, a trend not exhibited by the university and grocery wastes. In both feedstocks, pumpable waste resulted in a prolonged lag time. Also, T-tests indicate that there was a significant difference in methanation period for hotel waste. Specifically, pumpable hotel waste required a longer methanation time than the shredded hotel waste.

The relationship among food waste type, lag time, methanation period, peak methane production rate, and lipid content is presented in Figure 2 and Table A-4. Using the definition of lag and methanation time, the pumpable grocery store waste had a lag time of 2 days which was correlated with a relatively low methanation period, some of the highest methane production rates, and the lowest lipid content. In contrast, the pumpable hotel waste exhibited among the highest lag times and was correlated with the highest methanation periods, the lowest methane production rates, and the highest lipid content (Table A-4).

While there is considerable scatter in the trends in Figure 2, the food waste with the highest lipid content is correlated with the lowest maximum methane production rates and the lowest lipid content food waste is correlated with the highest maximum methane production rates. Also, food waste with the lowest lipid content was correlated with the lowest lag time. This result is consistent with a publication by Angelidaki and Batstone (2010) which indicates that lipids are a source for inhibitory compounds since long chain-fatty acids are formed from lipids during hydrolysis and these lipids can ultimately inhibit acetoclastic methanogens.

Figure 3 to Figure 6 and Table 7 exhibit the average cumulative methane yield of each reactor set and the data for each reactor are presented in Appendix Table A-1. T-Tests ($p > 0.05$) indicate that there was no significant effect of particle size on cumulative methane yield for any of the tested substrates although as noted above, the pumpable material exhibited an increased lag in the hotel and restaurant reactors. According to a T-Test ($p > 0.05$) the pumpable reactors exhibited a significantly lower standard deviation in

cumulative methane yield, as opposed to shredded reactors, which is most likely due to sample homogeneity (Table 7).

Methane yields were corrected for the volume of methane that could be attributed to the decomposed refuse used as an inoculum. This correction assumes that methane production from decomposed refuse is the same in the background and substrate reactors which were filled with a 7:3 volumetric mixture of well degraded MSW inoculum and food waste. To evaluate the importance of background methane production, the percentage of reactor methane produced that is attributable to the inoculum seed is presented in Table 9. This percentage ranged from about 1 to 16% which suggests that the assumption of equivalent behavior of the inoculum in background and substrate reactors is likely not a source of significant uncertainty in the calculated methane yields.

Lab scale decay rates of the different food waste types were calculated and are shown in Table 8. The calculated decay rates ranged from 21 to 36 yr⁻¹ and were all higher than the previously reported food waste decay rate of 15.02 yr⁻¹ (de la Cruz and Barlaz, 2010) which was based on only four replicate reactors containing one type of household food waste.

Table 7 Average cumulative methane yield from the four food wastes tested

Feedstock	Cumulative Methane Yield (mL CH ₄ /dry g)	Standard Deviation	Coefficient of Variation
Grocery Store Shredded	482.6	87.8	18.2
Grocery Store Pumpable	370.7	26.1	7.0
University Dining Hall Shredded	342.2	35.9	10.5
University Dining Hall Pumpable	382.9	27.8	7.3
Hotel and Conference Center Shredded	495.5	54.1	10.9
Hotel and Conference Center Pumpable	487.9	10.2	2.1
Restaurant Shredded	387.8	53.5	13.8
Restaurant Pumpable	419.1	6.5	1.6

Table 8 Lab scale decay rate from the four food wastes tested

Feedstock	k_{lab} (yr ⁻¹)	Standard Deviation
Grocery Store Shredded	28.66	6.55
Grocery Store Pumpable	36.55	5.44
University Dining Hall Shredded	25.75	10.85
University Dining Hall Pumpable	25.22	3.87
Hotel and Conference Center Shredded	26.67	5.78
Hotel and Conference Center Pumpable	21.34	6.08
Restaurant Shredded	28.59	5.23
Restaurant Pumpable	31.64	1.93

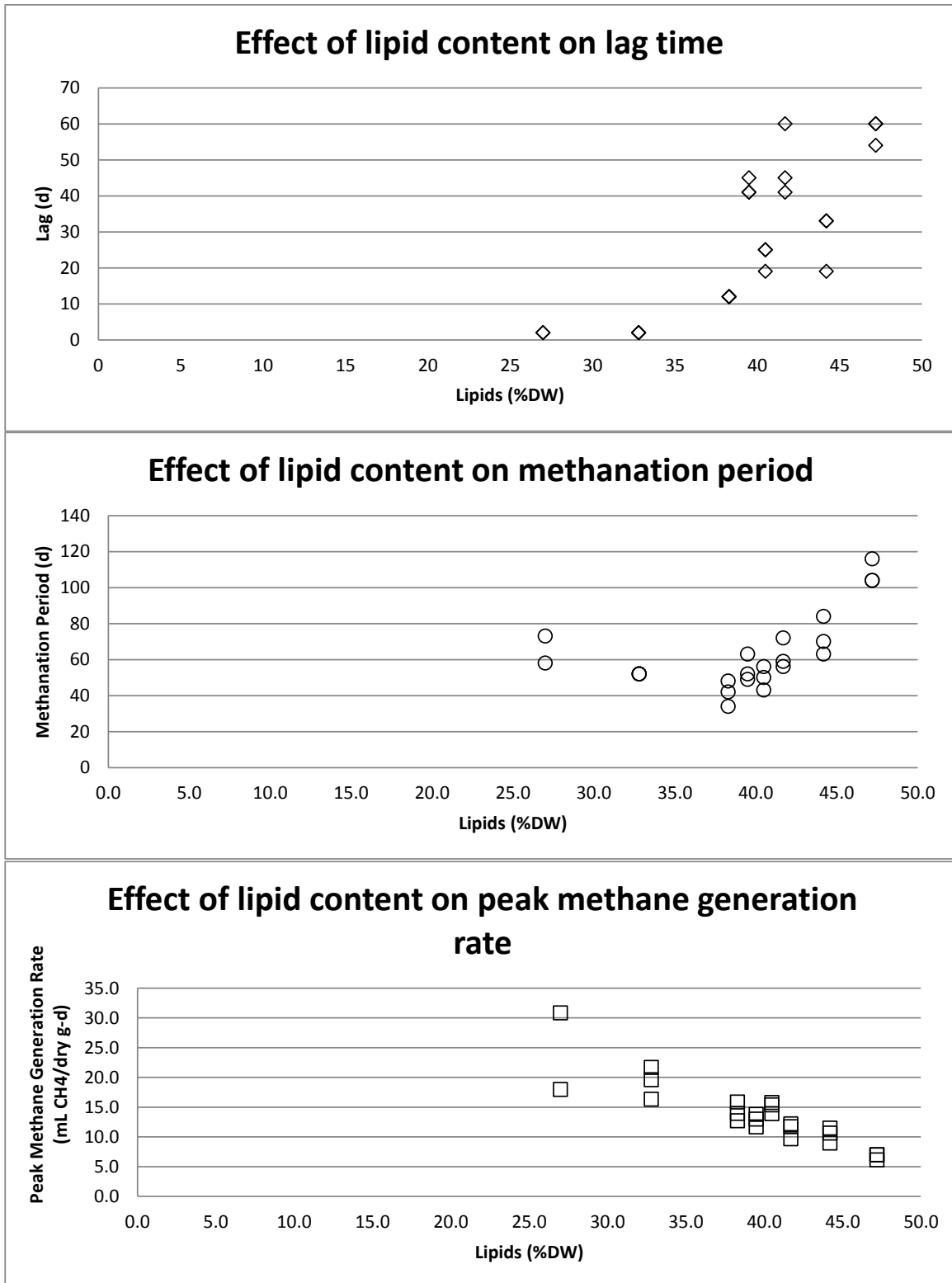


Figure 2 Correlation between lipids and lag time, methanation time, and peak methane generation rate in food waste reactor studies

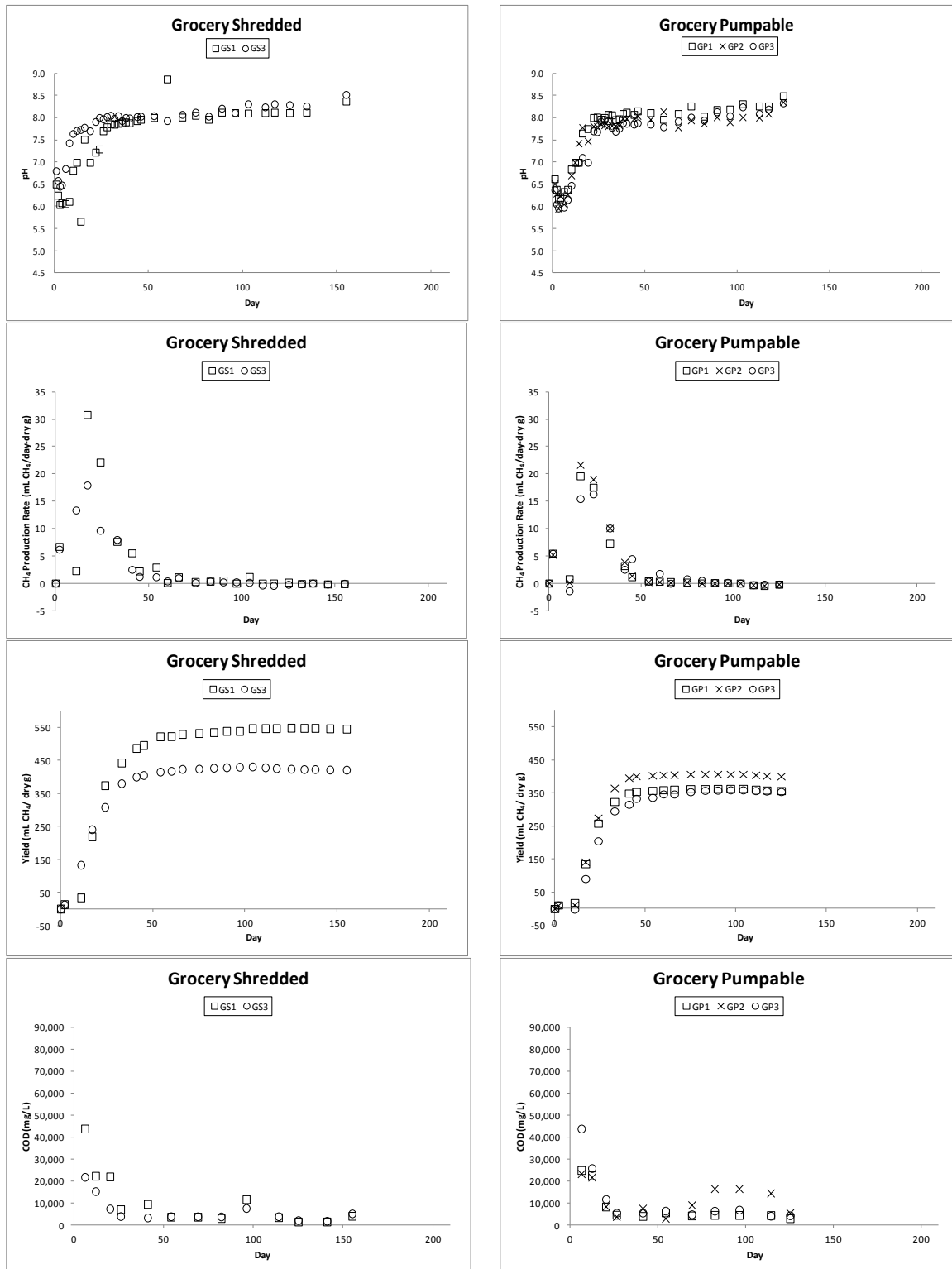


Figure 3 pH, methane production rate, cumulative methane yield, and COD plots for shredded and pumpable grocery store waste

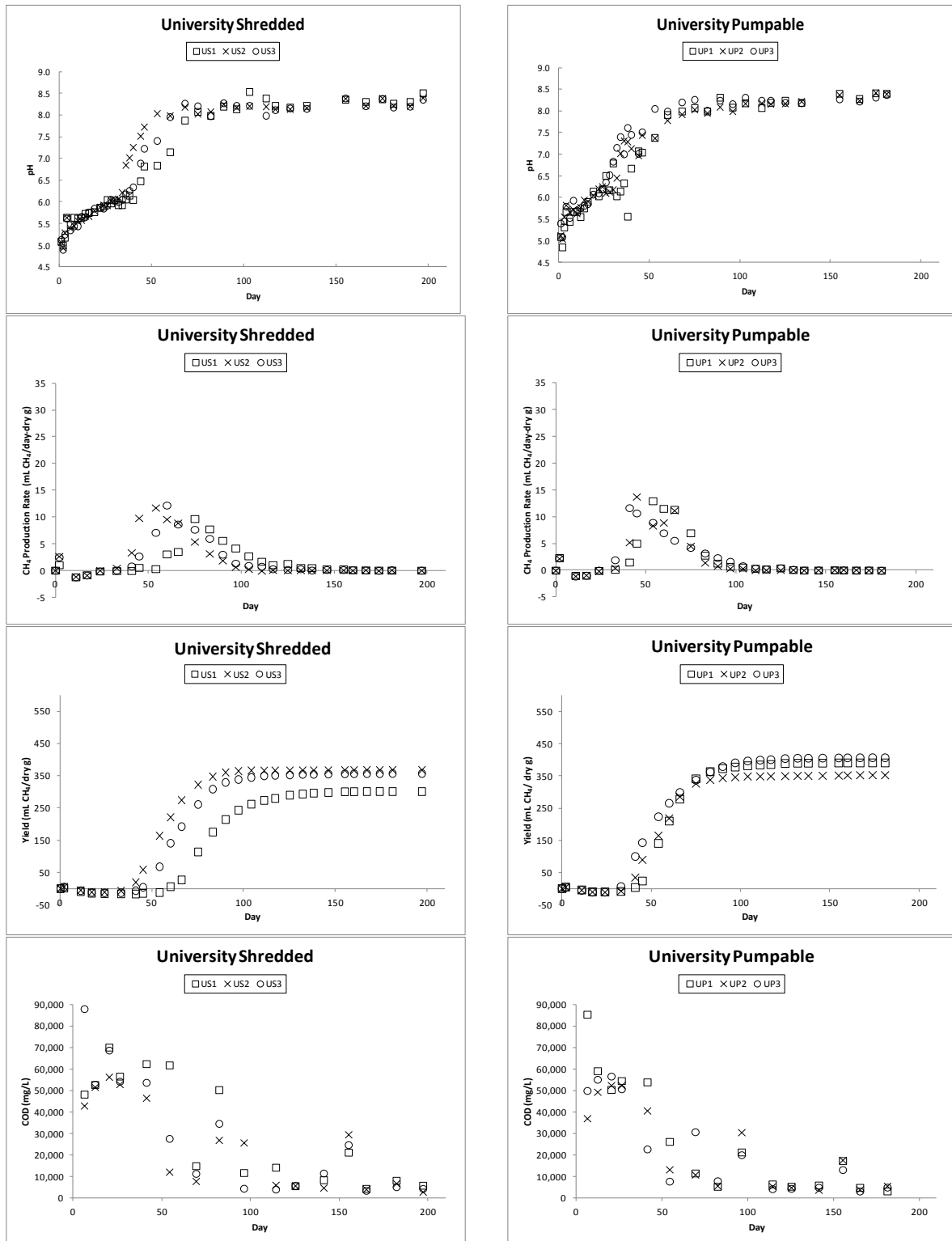


Figure 4 pH, methane production rate, cumulative methane yield, and COD plots for shredded and pumpable university dining hall waste

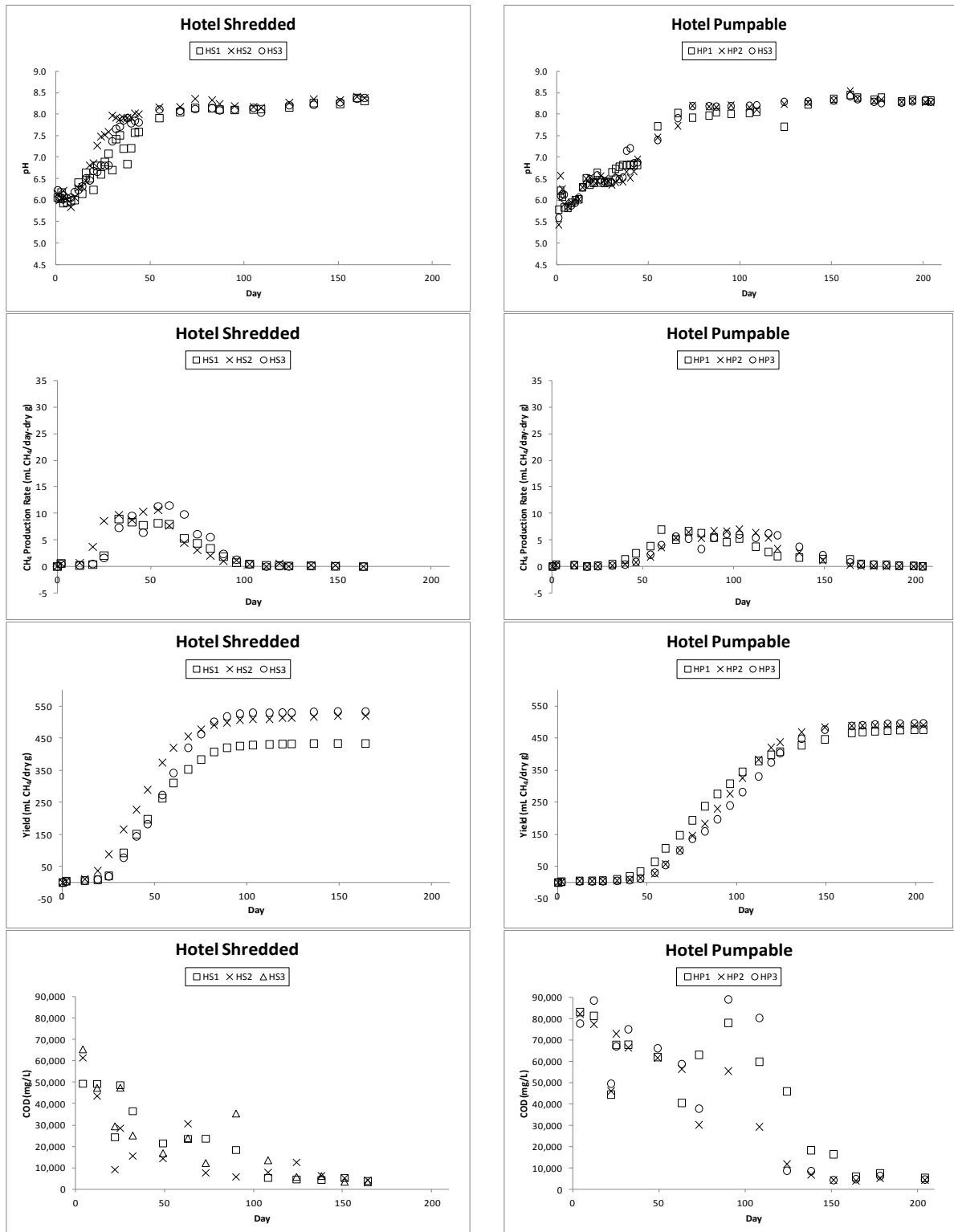


Figure 5 pH, methane production rate, cumulative methane yield, and COD plots for shredded and pumpable hotel and convention center waste

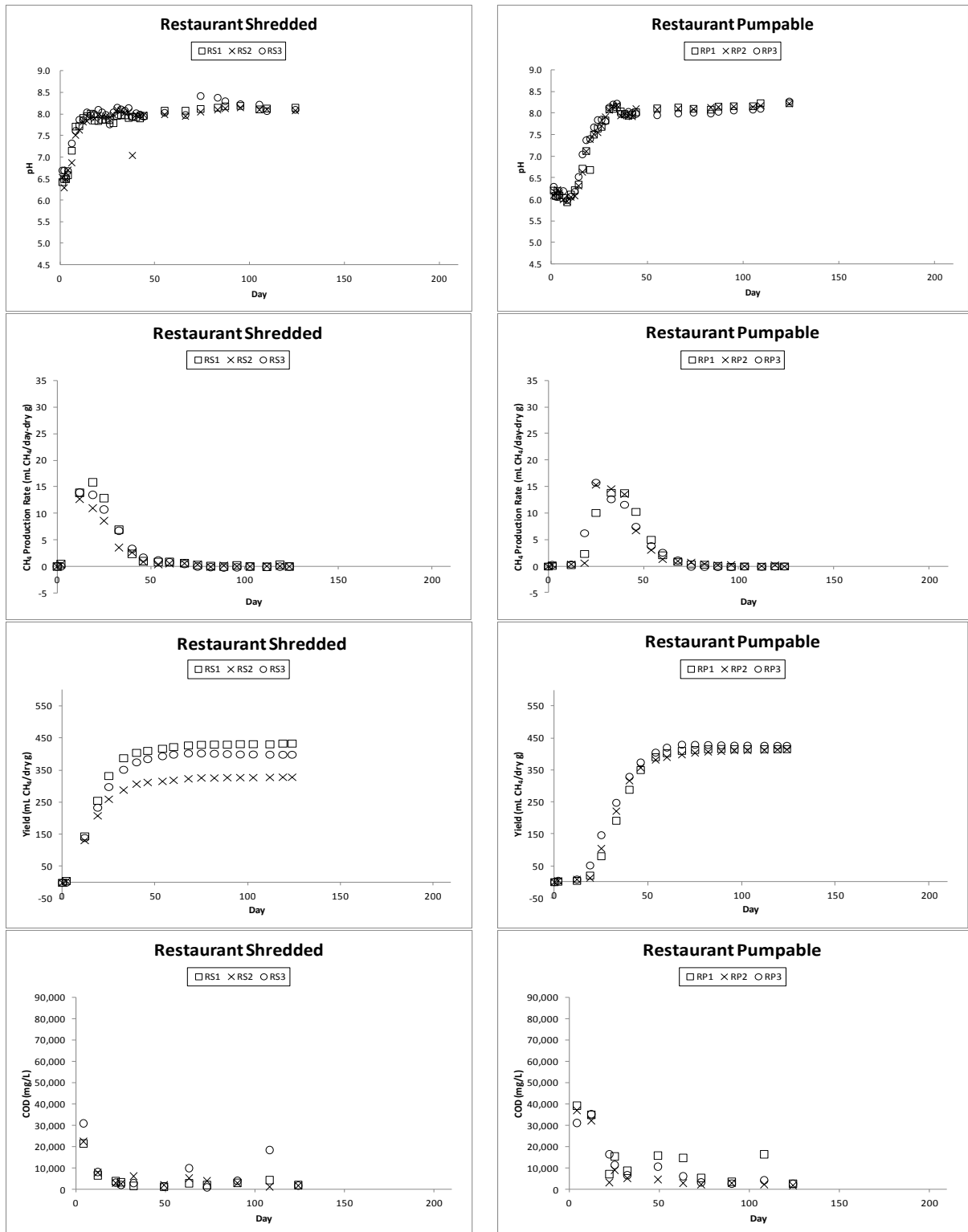


Figure 6 pH, methane production rate, cumulative methane yield, and COD plots for shredded and pumpable restaurant waste

Table 9 Total reactor methane attributed to inoculum seed for the four food wastes tested

Reactor		Total Methane Produced (L)	% Methane Due to Inoculum
MSW Inoculum Seed Control Blanks	B1	4.0	100.0
	B2	20.9	100.0
	B3	16.5	100.0
Grocery Store Shredded	GS1b	62.3	13.5
	GS3	51.9	16.1
Grocery Store Pumpable	GP1	53.0	16.5
	GP2	60.3	14.2
	GP3	52.6	15.8
University Dining Hall Shredded	US1	125.4	6.4
	US2	145.3	5.6
	US3	143.5	5.7
University Dining Hall Pumpable	UP1	160.5	5.1
	UP2	149.2	5.4
	UP3	168.0	5.0
MSW Inoculum Seed Control Blanks	B4	5.6	100.0
	B5	1.3	100.0
	B6	1.7	100.0
Hotel and Conference Center Shredded	HS1	115.5	2.1
	HS2	122.0	1.8
	HS3	147.7	1.4
Hotel and Conference Center Pumpable	HP1	175.9	1.2
	HP2	216.7	1.1
	HP3	223.7	1.1
Restaurant Shredded	RS1	56.5	4.2
	RS2	44.5	5.2
	RS3	53.3	4.4
Restaurant Pumpable	RP1	90.5	2.7
	RP2	86.6	2.6
	RP3	92.6	2.8

Leachate Quality

This section discusses reactor leachate quality including pH, COD, ammonia and phosphate along with methane production data to recognize trends in reactor performance.

An initial drop in pH was observed in each reactor (Figure 3 to Figure 6), which was presumably due to an accumulation of VFAs. During this acid phase of decomposition, the pH was lowest in the reactors that contained the university dining hall waste, with values below 5. In contrast, the pH did not decrease below 5.4 in the other reactor sets. The pH increased as a result of external pH neutralization which resulted in an increase in the methane production rate in all reactors. The reactor pH ranged broadly from 4.85 in university pumpable reactors to 8.52 in grocery shredded reactors.

The leachate soluble COD of each reactor was measured periodically throughout reactor operation. Figure 3 to Figure 6 exhibits the COD of each reactor. The COD was consistently higher in university and hotel food waste reactors; however the highest COD was exhibited in the hotel pumpable reactor set which started at approximately 80,000 mg COD/L. The lowest COD was measured in grocery and restaurant reactors, at an initial range of 21,800 to 43,800 mg COD/L. The final COD was no higher than 4,863 mg COD/L which can be attributable to recalcitrant humic matter. This decrease in COD concentration during the digestion process is attributed to the conversion of COD to biogas.

As shown in Figure 3 to Figure 6, when pH neutralized in each reactor set, the COD dramatically decreased due to consumption of the COD as part of the anaerobic process. This is coupled with the trend of the methane production rate which increased while the COD dramatically decreased once the pH was neutral.

Figure 7 and Figure 8 present the leachate $\text{NH}_3\text{-N}$ and PO_4 content of each reactor. Data are presented for three time points for each reactor and the sampling points correspond to reactor startup, peak methane generation, and reactor shutdown. These sampling dates differ for each reactor set because each substrate exhibited a unique methane production rate period as shown in Figure 3 to Figure 6. The data are also presented in Table A-2 and A-3.

Each reactor maintained sufficient nutrient levels of at least 5 mg of P/L and 100 mg of N/L (Eleazer et al., 1997) for proper microorganism growth throughout reactor operation. However, hotel waste reactors exhibited $\text{NH}_3\text{-N}$ levels above 3,000 mg $\text{NH}_3\text{-N/L}$ throughout reactor life. Concentrations above 3,000 mg $\text{NH}_3\text{-N/L}$ can be strongly inhibitory which increases the expectance of a reactor to fail (McCarty, 1964). The term “strongly inhibitory” is relative and can vary depending on the digester system configuration.

The VFA content of the leachate in the grocery and hotel wastes were analyzed to evaluate whether there was evidence that the hotel reactors were inhibited at the end of their decomposition period. An accumulation of VFAs would be indicative of inhibition. Data for the VFA assay is presented in Table 10. T-Tests ($p > 0.05$) confirm that there is no significant difference in the accumulation of acetic acid in grocery and hotel shredded waste or grocery and hotel pumpable waste. A significant accumulation of VFAs in hotel reactors as opposed to grocery reactors would have indicated hotel reactor inhibition at the tail end of the anaerobic process which ultimately converts VFAs to CH_4 and CO_2 . Since this is not the case, the data implies that hotel waste reactors did not experience inhibition as speculated.

It is to be noted that reactor GP2 exhibited elevated concentrations of VFAs compared to other reactors. These results are not correlated with any other unusual reactor

parameter values for pH, methane production rate, cumulative yield, COD, NH₃-N, or PO₄ compared to the other reactors for the set.

In order to further evaluate whether reactors were inhibited, a BMP assay was performed. This BMP was run on composite samples of triplicate reactor digested solids. Data from this assay will indicate the methane potential of these digested solids. The methane potential of each triplicate reactor set will be compared to determine to what extent reactors did not reach full methane potential once the BMPs are complete.

Table 10 Reactor shutdown VFA concentrations

Reactor Leachate	Acetic (mg/L)	Propionic (mg/L)	i-Butyric (mg/L)	n-Butyric (mg/L)	i-Valeric (mg/L)	Valeric (mg/L)	i-Caproic (mg/L)	Hexanoic (mg/L)
GS1	345.5	ND	ND	ND	2.7	ND	ND	ND
GS3	135.8	ND	ND	ND	ND	ND	ND	ND
GP1	161.0	ND	ND	ND	ND	ND	ND	ND
GP2	586.5	ND	5.8	119.4	5.4	ND	ND	ND
GP3	148.2	ND	ND	ND	ND	ND	ND	ND
HS1	110.3	ND	ND	ND	2.7	ND	ND	ND
HS2	190.6	ND	ND	ND	3.2	ND	ND	ND
HS3	115.6	ND	ND	ND	ND	ND	2.3	ND
HP1	146.9	ND	ND	ND	ND	ND	2.7	ND
HP2	93.4	ND	ND	ND	ND	ND	ND	ND
HP3	118.9	ND	ND	ND	2.5	ND	ND	ND
Detect Limit	20	20	2	20	2	2	2	10

a. ND indicates concentrations so low they were not detected by the VFA assay

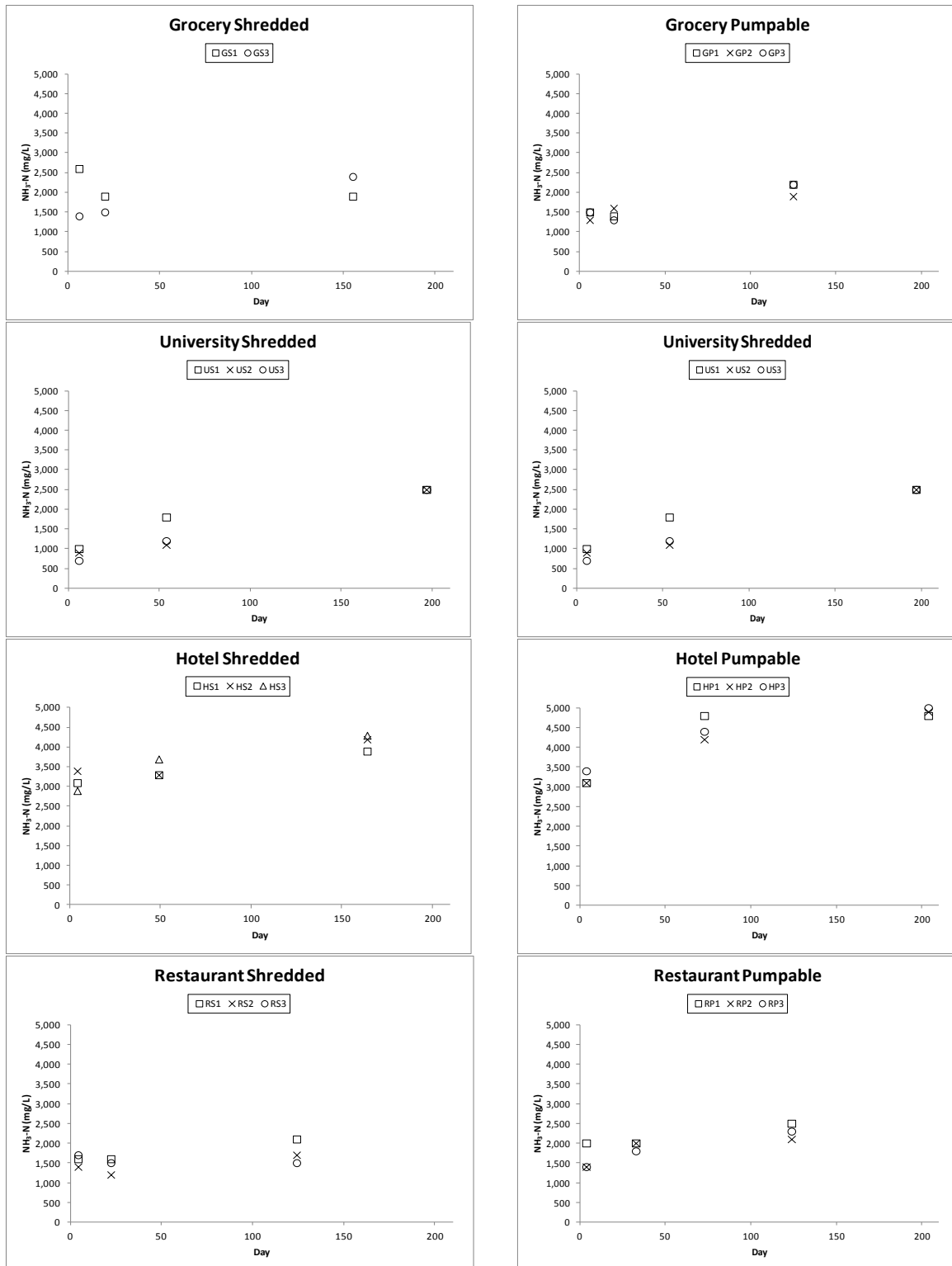


Figure 7 Leachate NH₃-N at reactor startup (first time point), peak methane generation (second time point), and reactor shutdown (third time point)

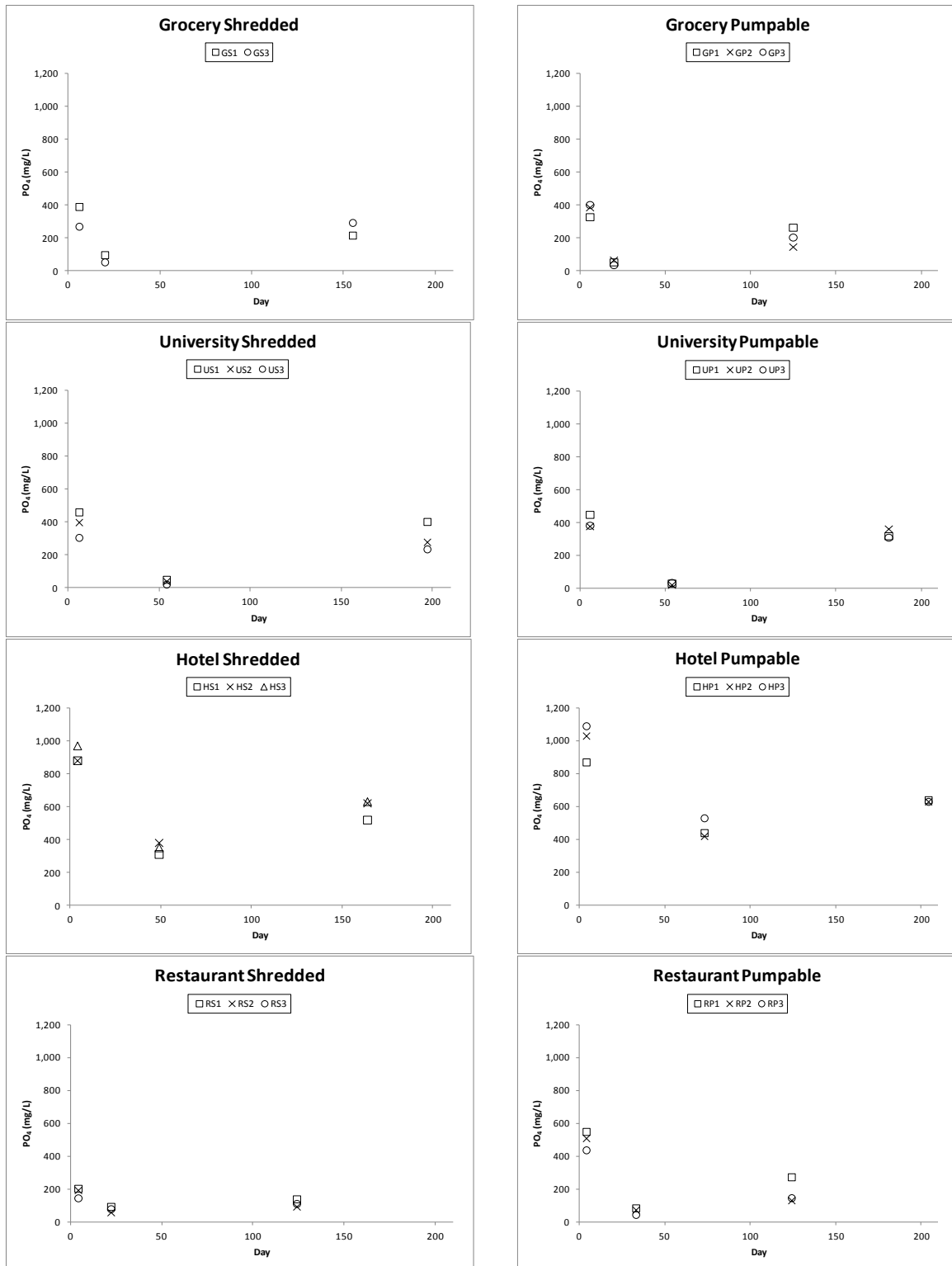


Figure 8 Leachate PO₄ at reactor startup (first time point), peak methane generation (second time point), and reactor shutdown (third time point)

Digested Solid Chemical Characterization

As shown in Table 11, cellulose, hemicellulose, and lignin, data have not all been determined. Once all of the raw feedstock and digested solid data is obtained, a mass balance described in the data analysis section will be used to determine the volume of methane that could be attributed to measured losses in cellulose, hemicellulose, starch, lipophilic materials, and protein.

Protein content was calculated by multiplying the organic nitrogen by a factor of 6.25, where organic nitrogen represents the total nitrogen on the solid phase after correction for the soluble ammonia nitrogen that was assumed to remain on the solid phase after drying the saturated solids removed from a reactor. This calculation assumes that the ammonia in the leachate remained with the solids after drying. As presented in Table 11, there are some negative values for protein, suggesting that the assumption that ammonia remained on the solids during drying is not correct. The pH of the reactors was generally in the range of 4.85-8.5 which is well below the pKa (9.25) for the $\text{NH}_4^+/\text{NH}_3$ system. Nonetheless, as some NH_3 volatilized more NH_4^+ was likely converted to NH_3 and then volatilized. Thus, another estimate of the protein content would simply be the measured N content on the solids multiplied by 6.25. It should be noted that the factor of 6.25 is applicable to biosolids and is uncertain as applied to the food waste system. The measured nitrogen may contain organic N associated with lignin. Protein values for the methane mass balance were represented as the upper protein limit of 6.25 multiplied by the N content of the solids.

Table 11 Average digested solid chemical characterization for each triplicate reactor set^b

Sample ^a	VS%	Starch%	Cellulose %	Hemicellulose %	Lignin%	Protein%	Lipids%	OrgC%	N%	Organic Component Balance
B	38.7	0.3	3.8	1.5	19.5	3.7	4.1	21.4	1.1	0.8
SD	4.8	0.1	0.5	0.3	2.7	0.8	0.3	1.4	0.2	0.0
GS	55.4	0.2	4.7	1.7	30.4	3.5	6.1	30.8	1.3	0.8
SD	1.2	0.0	1.0	0.3	1.4	0.7	0.4	1.6	0.1	0.0
GP	52.6	0.2	ND	ND	ND	3.4	5.7	30.9	1.4	0.9
SD	1.4	0.1	0.7	0.3	1.1	0.7	0.4	0.7	0.1	0.0
US	33.9	0.5	3.3	1.3	14.6	0.4	4.6	17.8	1.0	0.7
SD	3.7	0.1	0.4	0.4	1.2	0.2	0.8	2.5	0.1	0.0
UP	35.1	0.4	ND	ND	ND	0.6	4.8	18.6	1.1	0.4
SD	0.9	0.1	ND	ND	ND	0.3	0.9	1.9	0.1	0.0
B	44.7	0.8	ND	ND	ND	3.4	4.3	27.4	0.9	0.3
SD	2.1	0.5	ND	ND	ND	0.7	0.5	0.5	0.2	0.0
HS	49.7	0.2	ND	ND	ND	-2.4	6.2	31.1	1.1	0.2
SD	2.2	0.1	ND	ND	ND	2.1	0.6	2.4	0.2	0.0
HP	50.5	0.3	ND	ND	ND	-5.8	7.6	28.9	1.2	0.2
SD	1.2	0.0	ND	ND	ND	1.8	0.6	3.4	0.2	0.0
RS	33.9	0.5	ND	ND	ND	1.2	3.8	18.2	1.0	0.3
SD	3.4	0.1	ND	ND	ND	1.7	0.5	3.3	0.1	0.0
RP	35.8	0.4	ND	ND	ND	0.4	4.7	20.1	1.1	0.3
SD	2.0	0.1	ND	ND	ND	0.7	0.4	3.1	0.1	0.0

a. B is MSW Inoculum Seed Control Blanks, GS is Grocery Store Shredded, GP is Grocery Store Pumpable, US is University Dining Hall Shredded, UP is University Dining Hall Pumpable, HS is Hotel and Conference Center Shredded, HP is Hotel and Conference Center Pumpable, RS is Restaurant Shredded, and RP is Restaurant Pumpable food waste reactors

b. Results are reported in percent dry weight. Values are reported as averages, SD represents standard deviation, ND indicates that data has not yet been determined

CONCLUSIONS

1. On average, methane yields varied between about 340 and 500 ml CH₄/dry gm.
2. Cellulose assays capture starch as cellulose, thus over quantifying the cellulosic content of food waste.
3. There was no significant effect of particle size on cumulative methane yield for any of the tested substrates.
4. There was a significant difference in lag time for both hotel waste and restaurant waste due to particle size, a trend not exhibited by the university and grocery wastes. In both feedstocks, pumpable waste resulted in a prolonged lag time.
5. There was a significant difference in methanation period for hotel waste tested. Specifically, pumpable hotel waste required a longer methanation time than the shredded hotel waste.
6. Food waste with the highest lipid content was correlated with the lowest maximum methane production rates and the lowest lipid content food waste was correlated with the highest maximum methane production rates.
7. Food waste with the lowest lipid content was correlated with the lowest lag time.

RECOMMENDATIONS

1. High protein content food waste may affect protein loading thus causing ammonia toxicity.

This means that monitoring protein content of substrate chosen may be of importance.

2. This research indicates that lipids may be a food waste chemical component of concern when designing for digester efficiency due to the effect of lipids on methane production rates. This indicates that monitoring lipid content of substrate chosen may be of importance, however, further research on this topic is recommended in order to make a conclusive statement.

REFERENCES

- Agyeman, F.O., Tao, W., 2014. Anaerobic co-digestion of food waste and dairy manure: Effects of food waste particle size and organic loading rate. *Journal of environmental management* 133, 268–274.
- Angelidaki, I., Batstone, D.J., 2010. Anaerobic digestion: Process. *Solid Waste Technology & Management*, Volume 1 & 2 583–600.
- Browne, J.D., Murphy, J.D., 2013. Assessment of the resource associated with biomethane from food waste. *Applied Energy* 104, 170–177.
- Cho, J.K., Park, S.C., Chang, H.N., 1995. Biochemical methane potential and solid state anaerobic digestion of Korean food wastes. *Bioresource Technology* 52, 245–253.
- Christensen, T.H., 2011. *Solid waste technology & management*. Wiley Online Library.
- Davidsson, Å., Gruvberger, C., Christensen, T.H., Hansen, T.L., Jansen, J. la C., 2007. Methane yield in source-sorted organic fraction of municipal solid waste. *Waste Management* 27, 406–414.
- De la Cruz, F.B., Barlaz, M.A., 2010. Estimation of waste component-specific landfill decay rates using laboratory-scale decomposition data. *Environmental science & technology* 44, 4722–4728.
- De la Cruz, F.B., Yelle, D.J., Gracz, H.S., Barlaz, M.A., 2014. Chemical Changes during Anaerobic Decomposition of Hardwood, Softwood, and Old Newsprint under Mesophilic and Thermophilic Conditions. *Journal of agricultural and food chemistry* 62, 6362–6374.
- DEP, M., 2014. *Commercial Organic Materials Waste Ban Guidance for Businesses, Institutions, and Haulers*.
- EEA, 2009. *Effectiveness of waste management policies in the European Union*.
- Eleazer, W.E., Odle, W.S., Wang, Y.-S., Barlaz, M.A., 1997. Biodegradability of municipal solid waste components in laboratory-scale landfills. *Environmental Science & Technology* 31, 911–917.
- EPA, U., 2012. *Municipal Solid Waste Generation, Recycling, and Disposal in the United States: Facts and Figures for 2012*.
- Fdez-Güelfo, L., Álvarez-Gallego, C., Sales, D., Romero García, L., 2011. Determination of critical and optimum conditions for biomethanization of OFMSW in a semi-continuous stirred tank reactor. *Chemical Engineering Journal* 171, 418–424.

- Gray, D.M., Suto, P., Peck, C., 2008. Anaerobic Digestion of Food Waste. USEPA No. EPA-R9-WST-06 4.
- Hall, M.B., 2008. Determination of starch, including maltooligosaccharides, in animal feeds: Comparison of methods and a method recommended for AOAC collaborative study. *Journal of AOAC International* 92, 42–49.
- Hansen, K.H., Angelidaki, I., Ahring, B.K., 1998. Anaerobic digestion of swine manure: inhibition by ammonia. *Water research* 32, 5–12.
- Heo, N.H., Park, S.C., Kang, H., 2004. Effects of mixture ratio and hydraulic retention time on single-stage anaerobic co-digestion of food waste and waste activated sludge. *Journal of Environmental Science and Health, Part A* 39, 1739–1756.
- Lou, X.F., Nair, J., Ho, G., 2012. Effects of volumetric dilution on anaerobic digestion of food waste. *Journal of Renewable and Sustainable Energy* 4, 063112.
- Madigan, M.T., Martinko, J.M., Dunlap, P.V., Clark, D.P., 2008. *Brock Biology of microorganisms* 12th edn.
- McCarty, P.L., 1964. Anaerobic waste treatment fundamentals. *Public works* 95, 107–112.
- Mohan, S., Bindhu, B., 2008. Effect of phase separation on anaerobic digestion of kitchen waste. *Journal of Environmental Engineering and Science* 7, 91–103.
- Neves, L., Gonçalo, E., Oliveira, R., Alves, M., 2008. Influence of composition on the biomethanation potential of restaurant waste at mesophilic temperatures. *Waste management* 28, 965–972.
- Parkin, G.F., Owen, W.F., 1986. Fundamentals of anaerobic digestion of wastewater sludges. *Journal of Environmental Engineering* 112, 867–920.
- Qiao, W., Yan, X., Ye, J., Sun, Y., Wang, W., Zhang, Z., 2011. Evaluation of biogas production from different biomass wastes with/without hydrothermal pretreatment. *Renewable Energy* 36, 3313–3318.
- Ryba, S.A., Burgess, R.M., 2002. Effects of sample preparation on the measurement of organic carbon, hydrogen, nitrogen, sulfur, and oxygen concentrations in marine sediments. *Chemosphere* 48, 139–147.
- Staley, B.F., Xu, F., Cowie, S.J., Barlaz, M.A., Hater, G.R., 2006. Release of trace organic compounds during the decomposition of municipal solid waste components. *Environmental science & technology* 40, 5984–5991.

- U.S. Department of Agriculture, U.S.E.P.A.U.S.D. of E., 2014. Biogas Opportunities Roadmap.
- Wang, X., Padgett, J.M., Powell, J.S., Barlaz, M.A., 2013. Decomposition of forest products buried in landfills. *Waste management* 33, 2267–2276.
- Yazdani, R., 2010. Landfill-Based Anaerobic Digester Compost Pilot Project at Yolo County Central Landfill. For CalRecycle, Sacramento CA. Available online [www. calrecycle. ca. gov/Publications/Organics/2010002. pdf](http://www.calrecycle.ca.gov/Publications/Organics/2010002.pdf) [accessed 16/4/2012].
- Yazdani, R., Barlaz, M.A., Augenstein, D., Kayhanian, M., Tchobanoglous, G., 2012. Performance evaluation of an anaerobic/aerobic landfill-based digester using yard waste for energy and compost production. *Waste management* 32, 912–919.
- Zhang, R., El-Mashad, H.M., Hartman, K., Wang, F., Liu, G., Choate, C., Gamble, P., 2007. Characterization of food waste as feedstock for anaerobic digestion. *Bioresource technology* 98, 929–935.

APPENDICES

Appendix A Cumulative methane yield summary

Table A-1 Cumulative methane yield summary of triplicate reactor studies with the four food wastes tested

Reactor		Cumulative Methane Yield (mL CH ₄ /dry g)	Average Cumulative Methane Yield (mL CH ₄ /dry g)	SD ^a	CV ^c
MSW Inoculum Seed Control Blanks	B1	5.0	17.1	10.9	63.8
	B2	26.1			
	B3	20.2			
Grocery Store Shredded	GS1 ^b	544.7	482.6	87.8	18.2
	GS3	420.5			
Grocery Store Pumpable	GP1	357.1	370.7	26.1	7.0
	GP2	400.8			
	GP3	354.3			
University Dining Hall Shredded	US1	301.2	342.2	35.9	10.5
	US2	368.1			
	US3	357.3			
University Dining Hall Pumpable	UP1	390.3	382.9	27.8	7.3
	UP2	352.1			
	UP3	406.3			
MSW Inoculum Seed Control Blanks	B4	11.9	6.0	5.2	86.3
	B5	2.5			
	B6	3.6			
Hotel and Conference Center Shredded	HS1	433.6	495.5	54.1	10.9
	HS2	519.7			
	HS3	533.2			
Hotel and Conference Center Pumpable	HP1	476.6	487.9	10.2	2.1
	HP2	490.5			
	HP3	496.5			
Restaurant Shredded	RS1	434.4	387.8	53.5	13.8
	RS2	329.4			
	RS3	399.6			
Restaurant Pumpable	RP1	416.0	419.1	6.5	1.6
	RP2	414.6			
	RP3	426.6			

^a. SD represents standard deviation

^b. Reactor GS2 was discarded because of reactor gas leaking

^c. CV represents coefficient of variation

Appendix B Leachate NH3-N and PO3 data for reactor batch 1

Table A-2 Leachate NH3-N and PO3 data for reactor batch 1 at reactor startup (first time point), peak methane generation (second time point), and reactor shutdown (third time point)

		5/9/2014	5/23/2014	11/16/2014
	Day	6.00	20.00	197.00
B1	NH3-N	1100	800	1500
	PO4	197	112	240
B2	NH3-N	600	1000	1500
	PO4	123	94	268
B3	NH3-N	1000	1100	1300
	PO4	97	67	282
		5/9/2014	5/23/2014	10/5/2014
	Day	6.00	20.00	155.00
GS1	NH3-N	2600	1900	1900
	PO4	393	100	219
GS3	NH3-N	1400	1500	2400
	PO4	273	56	296
		5/9/2014	5/23/2014	9/5/2014
	Day	6.00	20.00	125.00
GP1	NH3-N	1500	1400	2200
	PO4	331	56	267
GP2	NH3-N	1300	1600	1900
	PO4	389	69	149
GP3	NH3-N	1500	1300	2200
	PO4	405	39	207
		5/9/2014	6/26/2014	11/16/2014
	Day	6.00	54.00	197.00
US1	NH3-N	1000	1800	2500
	PO4	463	53	405
US2	NH3-N	900	1100	2500
	PO4	401	42	281
US3	NH3-N	700	1200	2500
	PO4	308	24	238
		5/9/2014	6/26/2014	10/31/2014
	Day	6.00	54.00	181.00
UP1	NH3-N	900	1400	2600
	PO4	448	30	318
UP2	NH3-N	800	1700	2500
	PO4	377	21	361
UP3	NH3-N	800	1400	2500
	PO4	382	34	309

Appendix C Leachate NH3-N and PO3 data for reactor batch 2

Table A-3 Leachate NH3-N and PO3 data for reactor batch 2 at reactor startup (first time point), peak methane generation (second time point), and reactor shutdown (third time point)

	8/3/2014	8/7/2014	8/28/2014	1/14/2015
	Day	4.00	25.00	164.00
B4	NH3-N	800	1200	1200
	PO4	29	77	204
B5	NH3-N	800	1000	900
	PO4	33	63	118
B6	NH3-N	1100	1000	1100
	PO4	65	89	256
		8/7/2014	9/21/2014	1/14/2015
	Day	4.00	49.00	164.00
HS1	NH3-N	3100	3300	3900
	PO4	880	310	519
HS2	NH3-N	3400	3300	4200
	PO4	880	380	621
HS3	NH3-N	2900	3700	4300
	PO4	970	350	631
		8/7/2014	10/15/2014	2/23/2015
	Day	4.00	73.00	204.00
HP1	NH3-N	3100	4800	4800
	PO4	870	440	640
HP2	NH3-N	3100	4200	4900
	PO4	1030	420	630
HP3	NH3-N	3400	4400	5000
	PO4	1090	530	630
		8/7/2014	8/25/2014	12/5/2014
	Day	4.00	22.00	124.00
RS1	NH3-N	1600	1600	2100
	PO4	204	94	140
RS2	NH3-N	1400	1200	1700
	PO4	194	59	94
RS3	NH3-N	1700	1500	1500
	PO4	146	80	112
		8/7/2014	9/5/2014	12/5/2014
	Day	4.00	33.00	124.00
RP1	NH3-N	2000	2000	2500
	PO4	550	85	274
RP2	NH3-N	1400	2000	2100
	PO4	510	74	132
RP3	NH3-N	1400	1800	2300
	PO4	438	45	147

Appendix D Lag time, methanation period, peak methane production rate, and lipid content in food waste reactors

Table A-4 Lag time, methanation period, peak methane production rate, and lipid content in food waste reactors

Reactor	Lag (d)	Methanation period (d)	Peak methane production rate (mL CH ₄ /g-d)	Lipid (%DW)
HP1	54	116	7.0	39.2
HP2	60	104	7.0	39.2
HP3	60	104	6.1	39.2
HS1	33	63	9.0	37.6
HS2	19	84	10.6	37.6
HS3	33	70	11.5	37.6
US1	60	72	9.7	29.5
US2	41	56	11.7	29.5
US3	45	59	12.2	29.5
RS1	12	42	15.9	29.5
RS2	12	34	12.7	29.5
RS3	12	48	13.9	29.5
RP1	25	43	13.9	29.4
RP2	25	50	15.4	29.4
RP3	19	56	15.8	29.4
UP1	45	52	13.0	29.0
UP2	41	49	13.8	29.0
UP3	41	63	11.7	29.0
GS1	2	73	30.8	18.4
GS3	2	58	17.9	18.4
GP1	2	52	19.6	17.4
GP2	2	52	21.7	17.4
GP3	2	52	16.3	17.4